STUDY AND MITIGATION OF RADIATION EFFECTS IN THE LHCb UNDERGROUND AREAS

R. Calà*, C. Bertone, B. Bradu, F. Cerutti, J.-P. Corso, S. Fiore, G. Lerner, M. Pezzetti, M. Solfaroli Camillocci, CERN, Geneva, Switzerland

Abstract

During the 2024 and 2025 LHC proton-proton runs, the LHCb experiment, following its upgrade, achieved a substantial increase in delivered luminosity compared to previous years, exceeding the level of 10 fb^{-1} per year. While this enhancement greatly expands LHCb's physics reach, it also leads to a marked rise in radiation levels in the experimental insertion region, originally designed for a significantly lower luminosity target. Throughout the 2024 p-p operation, several failures of electronic racks and cryogenic sensors, mostly attributed to single-event effects (SEEs), were observed around the LHCb cavern and caused tens of hours of LHC downtime.

This work presents a benchmarking of dedicated FLUKA simulations, used to quantify the radiation levels and identify possible mitigation measures, against measurements by the Battery Radiation Monitors (BatMons). The study guided the relocation of sensitive equipment and the installation of additional shielding in specific underground areas hosting critical electronics, effectively reducing radiation exposure during the remainder of Run-3. Finally, possible improvements for shielding are also discussed in view of Run-4.

INTRODUCTION

The LHC beauty (LHCb) experiment is designed as a forward spectrometer, with a geometry specifically chosen to detect particles at small angles relative to the beam axis [1]. With respect to the general-purpose detectors at the LHC, which surround the interaction point with a enclosed structure, the open layout of LHCb allows collision debris to escape to a larger extent. This configuration leads to significant radiation streaming into the experimental cavern and adjacent service galleries, posing a challenge for the protection of nearby equipment. Coherently, while meeting its specific operational requirements, LHCb was originally designed to operate at luminosities substantially lower than those of the more hermetic ATLAS and CMS detectors.

However, during Long Shutdown 2 (LS2), the detector underwent a major upgrade (Upgrade I) to significantly increase its statistical reach [2]. This upgrade has enabled LHCb to operate at a leveled instantaneous luminosity of $2 \cdot 10^{33}$ $cm^{-2}s^{-1}$ during Run-3 (2022–2026), a factor of ∼5 higher than in the pre-upgrade era. The 2024 proton run marked a milestone in this new operational regime, delivering a record integrated luminosity of 10.9 fb^{-1} [3], more than four times the previous annual record achieved in 2018 [4].

This unprecedented increase in luminosity has led to a marked rise of radiation levels within the LHCb insertion region (IR8). In this environment, stochastic phenomena known as Single-Event Effects (SEEs) represent the primary threat to commercial electronic system functionality, causing operational downtime despite being mostly non-destructive to the hardware itself. Since the probability of a SEE is directly proportional to the hadron flux, High-Energy Hadron equivalent (HEH-eq) fluence is adopted as the critical metric for radiation environment assessment from the radiation to electronics (R2E) point of view [5, 6]. HEH-eq fluence accounts for all hadrons with energies above 20 MeV as well as 0.2–20 MeV neutrons weighted by their energy-dependent SEE-induction probability relative to a reference electronic device. For an area to be considered R2E-safe, the annual HEH-eq fluence must not exceed $3 \cdot 10^6$ $cm^{-2}yr^{-1}$ [7].

The impact of this luminosity upgrade became evident during the 2024 proton run and persisted throughout 2025, with a significant fraction of R2E events occurring in IR8 [8]. Many of these events involved pressure sensors located in the LHCb experimental cavern which were mitigated at software level. On the other hand, failures affecting the cryogenics system in the UL84 gallery, in particular the Active Magnetic Bearings (AMB) and PLC racks, led to tens of hours of LHC downtime [9]. This work details the estimation and validation of radiation levels through Monte Carlo simulations and *in-situ* measurements, and the mitigation strategies implemented to protect the critical infrastructures in UL84, including the relocation of sensitive equipment and the design of new shielding walls.

SIMULATION SETUP

Monte Carlo simulations are an essential tool for predicting the implications of particle shower propagation through complex geometries. In this study, radiation levels were evaluated using the FLUKA code, a multi-purpose simulation package providing accurate modeling of particle interactions with matter [10–13]. The comprehensive FLUKA model of IR8 incorporates a full three-dimensional description of the beamline, the LHC tunnel, the LHCb detector and the experimental cavern [14, 15].

The simulations presented here assume the proton-proton crossing schemes and optics for both Run-3 and Run-4, with colliding beam energies of 6.8 TeV and 7 TeV, respectively [16, 17]. To reflect operational reality, the simulations consider the total integrated luminosity as equally shared between the two polarity configurations of the LHCb spectrometer.

The HEH-eq fluence was evaluated using a 3D Cartesian mesh with $20 \times 20 \times 20$ cm^3 voxels. This resolution was chosen to provide a suitable representation of the spatial

* roberto.cala'@cern.ch

Figure 1: Evolution of the shielding configuration implemented by three interventions to protect the AMB system rack from radiation streaming at the UL84 entrance.

distribution of radiation levels relative to the dimensions and positioning of the electronics racks.

RADIATION SHIELDING AND MONITORING FOR UL84 ELECTRONICS

First Intervention – YETS 2024–2025

To protect the electronic racks at the UL84 entrance, housing the AMB system, FLUKA simulations were instrumental in defining a mitigation strategy. The latter, implemented during the 2024–2025 Year-End Technical Stop (YETS), followed a two-fold approach: first, the affected rack was relocated approximately 80 cm deeper into the UL84 gallery; second, a 80 cm thick concrete shielding structure was installed at the gallery entrance, immediately adjacent to the rack (see left picture in Fig. 1) [8]. The main constraints for the relocation were the maximum allowable cable length and the requirement to avoid any obstruction of the transport path (delimited by yellow floor markings).

To characterize the radiation environment and validate the shielding effectiveness, several BatMons [18] were deployed at strategic locations. BatMons are wireless, battery-powered devices specifically designed for radiation monitoring in accelerator complexes. They provide measurements of HEH-eq and Thermal Neutron equivalent fluences, as well as Total Ionizing Dose (TID), by leveraging the radiation sensitivity of SRAM-based sensors.

According to FLUKA simulations, this first intervention significantly mitigated the radiation exposure of the most critical rack positions. Specifically, the HEH-eq fluence at the location of the most sensitive AMB sensor (close to the BatMon-82, see Fig. 2) was more than halved from $3.7 \cdot 10^7$ to $1.6 \cdot 10^7$ cm^{-2} / 10 fb^{-1}[1].

Second Intervention – TS1 2025

Despite the aforementioned mitigation, two R2E events occurred in June 2025 within the UL84 racks. One failure affected the AMB, while the other involved the PLC rack of the cryogenics system. The latter is located deeper in the

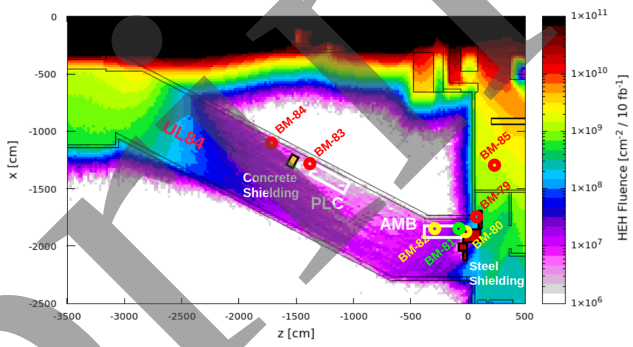

Figure 2: Top view of the simulated annual HEH-eq fluence in the UL84 gallery during Run-3, vertically averaged between -1.1 and 1.1 m. The map refers to the configuration with the two shielding walls installed in TS1 2025. The origin of the coordinate system corresponds to the collision point (IP8). The AMB and PLC racks and the installed BatMon monitors are indicated.

UL84 gallery, where it is also exposed to radiation streaming from the LHC tunnel (see Fig. 2). To address this vulnerability, a second intervention was carried out during the first Technical Stop (TS1) of 2025. The concrete shielding originally protecting the AMB rack was relocated deeper into UL84 to shield the PLC rack from the opposite tunnel side. Simultaneously, it was replaced with a larger steel shielding structure at the AMB rack location (see middle picture in Fig. 1), reaching a thickness of 160 cm in specific sections and partially encroaching upon the transport path marking.

However, the actual installation of the steel shielding presented a 45 cm gap relative to the UL84 wall compared to the nominal design. This unintended aperture allowed for radiation leakage, undermining the gains in overall shielding effectiveness and remaining uncorrected for the duration of the 2025 run.

The annual HEH-eq fluence levels in the concerned area, as simulated with FLUKA taking into account the actual shielding deployment featuring the aforementioned weakness, are presented in Fig. 2. The FLUKA predictions were benchmarked against BatMon measurements acquired from TS1 until October 9th 2025. Simulation results and data,

[1] The value of 10 fb^{-1} is taken as reference annual luminosity

Table 1: Comparison between HEH-eq fluences simulated by FLUKA and measured by different BatMons, normalized to an integrated luminosity of 10 fb^{-1}. The experimental data refer to the period from the end of TS1 to October 9th 2025, during which an integrated luminosity of 7.6 fb^{-1} was delivered to LHCb. The last column provides the ratio between simulation results and data. Statistical uncertainties of the FLUKA predictions range from 5% to 40% moving from high to low radiation locations.

BatMon ID	**FLUKA HEH Fluence** [cm^{-2} / 10 fb^{-1}]	**Measured HEH Fluence** [cm^{-2} / 10 fb^{-1}]	**Ratio**
BM-79	$3.7 \cdot 10^8$	$3.8 \cdot 10^8$	1.0
BM-80	$1.6 \cdot 10^8$	$9.5 \cdot 10^7$	1.7
BM-81	$2.7 \cdot 10^7$	$2.5 \cdot 10^7$	1.1
BM-82	$1.4 \cdot 10^7$	$1.1 \cdot 10^7$	1.3
BM-83	$2.6 \cdot 10^6$	$1.4 \cdot 10^6$	1.9
BM-84	$1.4 \cdot 10^7$	$1.4 \cdot 10^7$	1.1
BM-85	$1.3 \cdot 10^9$	$1.5 \cdot 10^9$	0.8

both rescaled to an integrated luminosity of 10 fb^{-1}, are reported in Table 1. Their ratio ranges from 0.8 to 1.9, demonstrating the reliability of the simulation framework. While the misalignment of the new steel shielding left the AMB rack exposed to a HEH-eq fluence of $\sim 1.4 \cdot 10^7$ cm^{-2} / 10 fb^{-1}, the wall on the other side of the PLC rack deeper in the gallery successfully reduced the HEH-eq fluence at the latter from $\sim 1 \cdot 10^7$ down to $\sim 2 \cdot 10^6$ cm^{-2} / 10 fb^{-1}.

Third Intervention – YETS 2025–2026

The misalignment of the steel shielding at the UL84 entrance was fixed during the 2025–2026 YETS. In addition to this correction, further modifications were implemented, as illustrated by the right pictures in Fig. 1: the gap between the shielding wall and the US85 cavern wall was partially filled with steel bricks and the overall length of the structure was reduced to avoid any obstruction of the yellow-marked transport path.

According to FLUKA simulations, the resulting shielding configuration is expected to reduce the HEH-eq fluence at the most fault-prone AMB sensor down to $1.0 \cdot 10^7$ cm^{-2} / 10 fb^{-1}. A new benchmarking campaign will be conducted for the 2026 proton run to validate the effectiveness of the current solution.

MITIGATION STRATEGIES FOR RUN-4

The shielding installed at the UL84 entrance was conceived as an urgent measure to protect the AMB rack for the rest of Run-3. However, further optimizations to minimize the risk of SEEs in the cryogenic sensors are currently under discussion for Run-4 (starting in 2030). Any long-term shielding solution must comply with two main logistic constraints: it must not extend beyond the markings delimiting the transport path and it must avoid placement directly on top of the floor ventilation gratings, differently from the current temporary setup.

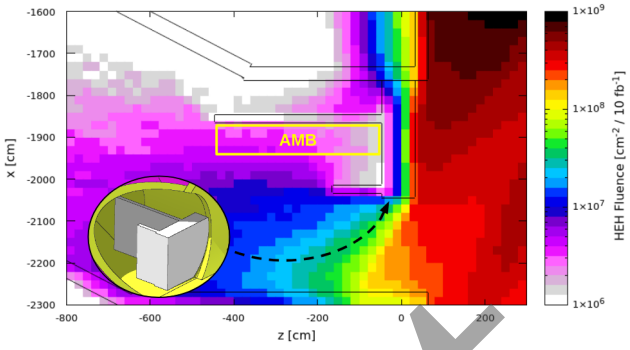

Figure 3: Top view of the simulated annual HEH-eq fluence at the UL84 entrance during Run-4, vertically averaged between -1.1 and 1.1 m. The map refers to an optimized shielding configuration featuring a 20 cm thick steel layer behind the AMB rack, as displayed by the FLUKA 3D model in the bottom-left corner inset.

One promising solution evaluated through FLUKA simulations involves protecting the AMB rack from radiation streaming from the LHCb detector by installing a 20 cm thick steel shielding at the rear of the rack, as shown in Fig. 3. This configuration would potentially reduce the HEH-eq fluence at the rack location down to about $4 \cdot 10^6$ cm^{-2} / 10 fb^{-1}.

In addition to these localized shielding strategies, the complete relocation of the AMB and PLC racks to radiation-free zones farther from the detector, such as the UA galleries or surface buildings, is being considered, with a detailed cost-benefit analysis currently ongoing to assess the feasibility of this option.

CONCLUSION

The record luminosity achieved by LHCb in Run-3 has significantly increased the radiation-induced risk for nearby electronics. This work demonstrates that the synergy between FLUKA simulations and *in-situ* monitoring via the BatMon system allowed for effectively diagnosing and mitigating radiation-induced failures in the vicinity of the experimental cavern.

The interventions implemented in the UL84 gallery addressed critical failures, reducing the High-Energy Hadron equivalent fluence at the most sensitive AMB sensor by almost a factor of 4, down to $\sim 1.0 \cdot 10^7$ cm^{-2} / 10 fb^{-1}. Moreover, the same quantity was lowered to $\sim 2 \cdot 10^6$ cm^{-2} / 10 fb^{-1} at the PLC rack, bringing it within the radiation-safe limit. Despite unavoidable approximations in the simulated geometry, the FLUKA model yielded a simulation-to-measurement ratio between 0.8 and 1.9 over a 3-order-of-magnitude range, proving its high level of reliability.

While improved localized shielding can further reduce the relevant particle fluence in the short term, the relocation of sensitive electronics to radiation-free zones is being evaluated as the most robust solution for Run-4.

REFERENCES

[1] LHCb Collaboration, "The LHCb Detector at the LHC", *J. Instrum.*, vol. 3, p. S08005, 2008. doi:10.1088/1748-0221/3/08/S08005

[2] LHCb Collaboration, "Framework TDR for the LHCb Upgrade", CERN, Geneva, Switzerland, Rep. CERN-LHCC-2012-007, 2012. https://cds.cern.ch/record/1443882

[3] C. Pralavorio, "Record data for the LHC in 2024", *CERN News*, Nov. 2024. https://home.cern/news/news/accelerators/record-data-lhc-2024

[4] LHC Programme Coordination (LPC) website, https://lpc.web.cern.ch

[5] K. Røed *et al.*, "Method for measuring mixed field radiation levels relevant for SEEs at the LHC", *IEEE Trans. Nucl. Sci.*, vol. 59, no. 4, pp. 1040–1047, 2012. doi:10.1109/TNS.2012.2183677

[6] M. Cecchetto *et al.*, "SEE Flux and Spectral Hardness Calibration of Neutron Spallation and Mixed-Field Facilities", *IEEE Trans. Nucl. Sci.*, vol. 66, no. 7, pp. 1532–1540, 2019. doi:10.1109/TNS.2019.2908067

[7] G. Lerner *et al.*, "Radiation level specifications for HL-LHC", CERN, Geneva, Switzerland, Rep. 2302154 / Rep. LHC-N-ES-0001, 2020.

[8] D. Söderström *et al.*, "Radiation monitoring and R2E performance in the LHC during the 2024 proton run", in *Proc. IPAC'25*, Taipei, Taiwan, Jun. 2025, pp. 3006–3009. doi:10.18429/JACoW-IPAC2025-THPS024

[9] M. Pezzetti, "Control of large helium cryogenic systems: a case study on CERN LHC", *EPJ Techn. Instrum.*, vol. 8, no. 6, 2021. doi:10.1140/epjti/s40485-021-00063-w

[10] FLUKA website, https://fluka.cern

[11] C. Ahdida *et al.*, "New Capabilities of the FLUKA Multi-Purpose Code", *Front. Phys.*, no. 9, p. 788253, 2022. doi:10.3389/fphy.2021.788253

[12] G. Battistoni *et al.*, "Overview of the FLUKA code", *Ann. Nucl. Energy*, vol. 82, pp. 10–18, 2015. doi:10.1016/j.anucene.2014.11.007

[13] G. Hugo *et al.*, "Latest FLUKA developments", *EPJ N Nucl. Sci. Technol.* 10, 2024. doi:10.1051/epjn/2024023

[14] A. Donadon *et al.*, "FLAIR3 – recasting simulation experiences with the Advanced Interface for FLUKA and other Monte Carlo codes", *EPJ Web Conf.*, vol. 302, 11005, 2024. doi:10.1051/epjconf/202430211005

[15] A. Mereghetti *et al.*, "The FLUKA LineBuilder and Element Database", in *Proc. IPAC'12*, New Orleans, LA, USA, May 2012, pp. 2687–2689

[16] S. Fartoukh *et al.*, "LHC Configuration and Operational Scenario for Run 3", CERN, Geneva, Switzerland, Rep. CERN-ACC-2021-0007, 2021

[17] A. Ciccotelli *et al.*, "Energy deposition studies for the LHCb insertion region of the CERN Large Hadron Collider", *Phys. Rev. Accel. Beams*, vol. 26, p. 061002, 2023. doi:10.1103/PhysRevAccelBeams.26.061002

[18] A. Zimmaro *et al.*, "Testing and validation methodology for a radiation monitoring system for electronics in particle accelerators", *IEEE Trans. Nucl. Sci.*, vol. 69, pp. 1642–1650, 2022. doi:10.1109/TNS.2022.3158527